# Measurement of $^1H(n,\gamma)^2H$ reaction cross section at a comparable $M1/E1$ strength

Y. Nagai, T. S. Suzuki, T. Kikuchi, T. Shima, T. Kii, and H. Sato
*Department of Applied Physics, Tokyo Institute of Technology, O-okayama, Meguro, Tokyo 152, Japan*

M. Igashira
*Research Laboratory for Nuclear Reactors, Tokyo Institute of Technology, O-okayama, Meguro, Tokyo 152 Japan*
(Received 29 July 1997)

The cross section of the $p(n,\gamma)d$ reaction was directly measured for the first time at $E_n=550$ keV, where the theoretical $E1$ transition strength is comparable to the $M1$ strength. It was determined accurately to be 35.2 (24) $\mu$b, and it agrees with the theoretical one which includes the meson-exchange currents. In this work, a prompt discrete $\gamma$-ray detection method combined with a pulsed neutron beam and a newly developed Monte Carlo code was essential to obtain an accurate cross section. [S0556-2813(97)00612-2]

PACS number(s): 25.40.Lw, 25.10.+s, 29.30.Kv

## I. INTRODUCTION

The low-energy neutron-capture reaction by a proton is one of the important reactions in both nuclear physics [1] and nuclear astrophysics [2]. In nuclear physics, the $n$-$p$ two-body system is the conceptually simple and solvable one, and therefore, the reaction has been expected to provide valuable information about the nucleon-nucleon interaction, the wave function of the deuteron, and the electromagnetic properties of nucleons. Actually, the critical role of meson-exchange currents (MEC's) [3] was revealed for the first time in the measured $p(n,\gamma)d$ reaction cross section for thermal neutrons [4]. Here the thermal neutron-capture reaction proceeds via the $s$-wave capture with the $M1$ transition mostly between an $^1S_0$ $T=1$ scattering state and the deuteron ground state with $^3S_1$and $^3D_1$ components of $T=0$, and thus, a sizable effect of isovector MEC's was observed [3]. Since the measurement of the thermal neutron capture, the experimental studies of the $p(n,\gamma)d$ $\{d(\gamma,p)n\}$ reaction were performed mostly at a higher neutron $\{\gamma$-ray$\}$ energy [5] to investigate various effects, such as $\rho$ and $\omega$ exchanges and relativistic corrections to the impulse approximation (IA) [6], while the theoretical calculations were carried out on the total, differential cross section and the polarization of the emitted nucleon in the $d(\gamma,p)n$ reaction from low energy up to more than 100 MeV [7]. In the low-energy region $E_\gamma$ $<20$ MeV, it has been suggested that there are discrepancies between theory and experiment as discussed below. Namely, the polarization $P(n)$ and angular distribution of $P(n)$ of the neutron from the $d(\gamma,p)n$ reaction were measured in the $\gamma$-ray energy region $6<E_\gamma<13$ MeV [8] and at $E_\gamma=2.75$ MeV [9], respectively, and they differ from the theoretical values which include the contribution of MEC's. The analyzing power was also measured for the $p(n,\gamma)d$ reaction using polarized neutrons of 6 and 13.4 MeV, and the results differ from the theory [10], while the measured angular distribution of the neutron at $E_\gamma=2.75$ MeV is in good agreement with the theory [11]. In these situations of experiment and theory, and in view of the importance of the reaction, it would be worthwhile to carry out a new experiment on the problem. Here it should be mentioned that the measurement of the cross section $\sigma(n,\gamma)$ of the $p(n,\gamma)d$ $\{d(\gamma,p)n\}$ reaction has not been well studied in the low-energy region, mostly due to the experimental difficulty as discussed later. Hence it would be interesting if one could measure the $\sigma(n,\gamma)$ at low energy and shed light on the problem. In nuclear astrophysics, the $p(n,\gamma)d$ reaction is known to create all deuterium in the early universe. The cross section $\sigma(n,\gamma)$, therefore, is necessary to estimate the production yields of primordial light elements [2]. Since it was not measured at the astrophysically relevant energy of between 10 and 600 keV, it was derived from the cross section $\sigma(\gamma,p)$ of the $d(\gamma,p)n$ reaction, which was estimated by the effective range theory [12]. Recently new calculations of $\sigma(n,\gamma)$ were made by Hale *et al.* [13], Smith *et al.* [14], and Sato *et al.* [15]; their values agree with each other within 5% deviation, although they differ from the old one [12] as noted in Refs. [14] and [15]. Here it should be mentioned that although theoretical work of $\sigma(\gamma,p)$ was made in the threshold region of the deuteron photodisintegration [7], the experimental value was not available for a long time, and thus in order to estimate the production yield of the primordial light elements the old value [12] was used until quite recently [14]. The authors [13,14] obtained the cross section by fitting the existing data with a polynomial expansion, while Sato *et al.* performed a theoretical calculation by including the MEC's, isobar currents, and pair currents: The result is shown in Fig. 1 as a function of the neutron energy, where $M1$(IA) is the $M1$ strength calculated without the MEC's effects. It is interesting to note that the MEC's enhance the $M1$ strength by about 10% in the $\sim$keV neutron region. According to the theory, the $M1$ strength decreases in proportion to $(E_n)^{-1/2}$ up to a few keV and decreases significantly for neutrons $E_n>100$ keV; it is about 94% and 59% at $E_n=10$ and 100 keV, respectively, of the extrapolated value of the measured thermal capture cross section assuming a $1/v$ law, while the $E1$ transition strength, connecting between a $^3P_1$ $T=1$ scattering state populated by a $p$-wave neutron capture and the deuteron ground state, increases roughly in proportion to $(E_n)^{1/2}$, and, thus, it becomes comparable to the $M1$ strength

 

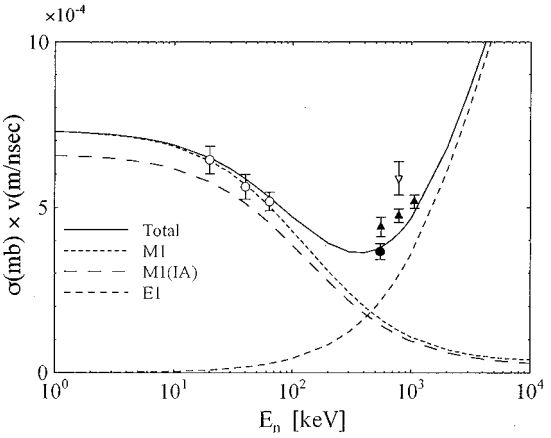


FIG. 1. The dependence of the calculated $p(n,\gamma)d$ reaction cross section $\sigma$ times the neutron velocity $v$ on the neutron kinetic energy (laboratory). The solid line represents the total cross section, the dotted line (short) shows the $M1$ strength by taking into account the meson-exchange currents, and the dashed line is the $M1$ strength by the impulse approximation (IA). The dotted line (long) is the $E1$ strength. The solid and open circles are the measured ones in the present and previous experiments. The solid triangle is the measured one [16].

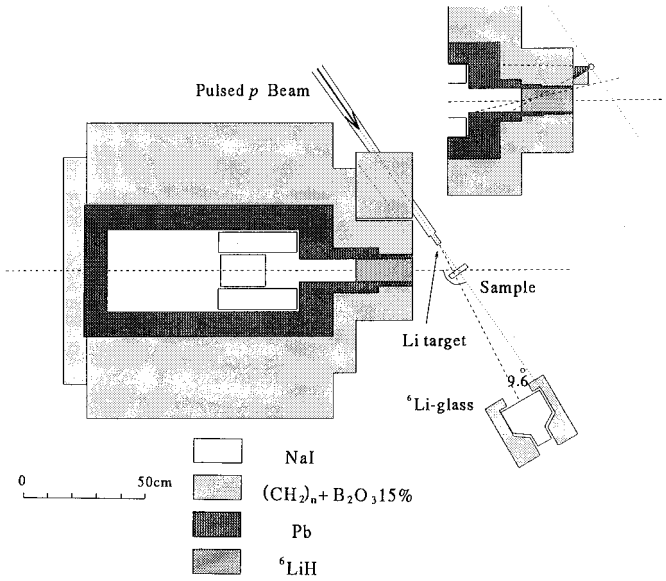


FIG. 2. Schematic view of the experimental setup. In order to attenuate the intense high-energy $\gamma$ ray and neutron from both the $^7$Li$(p,\gamma)^8$Be and $^7$Li$(p,n)^7$Be reactions, we tried to use many shadow bars with various shapes and combinations of Pb and borated paraffin.

at $E_n \sim 500$ keV, and is then dominant at $E_n \geqslant 2$ MeV. Because of these features of the $M1$ and $E1$ strength, the total capture cross section is predicted to have the minimum value at $E_n \sim 1$ MeV. The theory is in good agreement with the cross section measured for neutrons above 14 MeV, but it deviates by about 15% from the measured cross section of the $d(\gamma,p)n$ reaction by using the $\gamma$ ray of between 2.5 and 2.75 MeV [16], corresponding to neutron energies of 550 and 1080 keV, as shown in Fig. 1. Since that time, the cross section has not been measured in the above neutron ($\gamma$-ray) energy region.

In view of these circumstances of both nuclear physics and nuclear astrophysics, it would be quite important to measure directly the cross section $\sigma(n,\gamma)$ at low energy, and therefore, in this study we aimed at measuring it at $E_n = 550$ keV precisely. Here it should be mentioned that quite recently the cross section was measured in the neutron energy region between 10 and 80 keV [17] and it agrees well with the theory.

## II. EXPERIMENTAL PROCEDURE

The neutron-capture cross section by a light nucleus is very difficult to accurately measure at low $E_n$ of ~keV, because of the low incident neutron intensity ($\sim 5 \times 10^3$/cm$^2$/s/keV), the small cross section ($\sim 10^2$ $\mu$b), and a lot of thermal neutrons having $\sim 10^3$ times larger capture cross section than keV neutrons. Therefore, in order to obtain a sufficient $\gamma$-ray yield with a good signal-to-noise ratio, one has to use a large amount of a (solid) sample and develop the measuring system, which can discriminate a weak true signal from huge background. In the case of a solid hydrogen (H) sample, the measurement becomes especially difficult due to the following two reasons. First, there are many materials containing H atoms around a $\gamma$-ray detector and they produce an intense 2.22-MeV $\gamma$-ray background signal after capturing scattered and/or thermalized neutrons. Second, there are multiple-scattering effects of incident neutrons in the solid H sample, which cause uncertainties in determining the cross section, if the corrections of the scattering were not properly made. Here the fact that the masses of the neutron and proton are same is critical (discussed later). In order to overcome these problems, we used the prompt discrete $\gamma$-ray detection method combined with pulsed neutrons and a newly developed Monte Carlo code TIME-MULTI [18]. They were shown to be powerful for measuring the cross sections of an order of 200 $\mu$b at low $E_n$ [17]. In this experiment, we improved the sensitivity of the measuring system further, since the cross section predicted is as small as about 40 $\mu$b [15], and also the neutrons emitted (scattered) from the Li target (the sample) produced much background, making the signal-to-noise ratio worse as discussed later.

The experiment was carried out using 550-keV pulsed neutrons produced by the $^7$Li$(p,n)^7$Be reaction. The 2.3-MeV pulsed protons of 1.5 ns width, provided by the 3.2-MV Pelletron Accelerator of the Research Laboratory for Nuclear Reactors at the Tokyo Institute of Technology, were bombarded on a thin layer of metallic Li; an average beam current of 13 $\mu$A was obtained at a repetition rate of 4 MHz. Lithium was evaporated onto a copper disk, which was cooled by a kind of atomizer to prevent Li from evaporating. A schematic view of the experimental setup is shown in Fig. 2. The incident neutron energy spectrum was measured by a time-of-flight (TOF) method with an efficiency calibrated $^6$Li-glass scintillation counter (without a captured sample) [19]. It was set at 4.5 m away from the Li target at an angle of 9.6° with respect to the proton beam direction (hereafter, any angle is defined in the same way). Thus the averaged energy spectrum could be obtained on a capture sample because of the reaction kinematics, and it is shown in Fig. 3. Prompt $\gamma$ rays from a capturing sample were detected by an

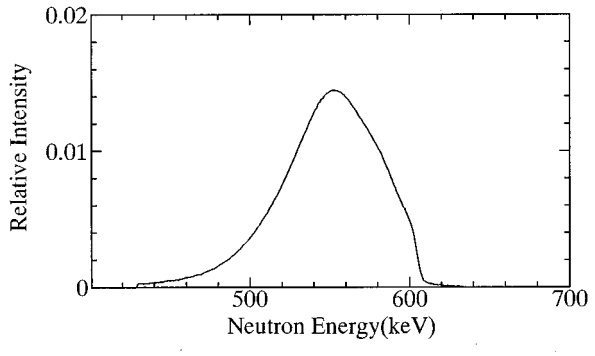


FIG. 3. Neutron energy spectrum measured by a TOF method with a $^6$Li-glass scintillation counter.

anti-Compton NaI(Tl) spectrometer [20], which comprised a central NaI(TI) detector with a diameter of 15.2 cm and a length of 20.3 cm, as well as an annular one with a thickness of 6.4 cm and a length of 35.6 cm. The captured events detected by the central NaI(Tl) detector were stored on a hard disk by a list model (TOF vs pulse height) [21]. The neutron energy captured by a sample was determined by using the TOF method, where both the $\gamma$-ray signal detected by the central NaI(Tl) detector and time-pick off signal from the pulsed proton beam were used as start and stop signals, respectively. Two polyethylene samples with thicknesses of 6.3 and 10.5 mm, and gold (Au) with thickness of 1 mm were used, respectively. The neutron transmissions of these polyethylene samples were 66% and 51%, respectively. The gold was used for normalizing the $\gamma$-ray yields of the hydrogen sample with those of Au, since the absolute capture cross section has been known accurately within an uncertainty of 3% [22]. These samples were placed at 19.8 cm away from the Li target at an angle of 0°. This distance was necessary to separate the reaction $\gamma$-ray event due to the sample from that of the $^7Li(p,\gamma)^8Be$ reaction at the neutron target by the TOF method with the central NaI(Tl) detector. Here the high-energy $\gamma$ rays up to 17 MeV from the $^7Li(p,\gamma)^8Be$ reaction entered the detector through the thick Pb covering the NaI(Tl) spectrometer. The measurements were carried out cyclically on polyethylene, Au, and blank samples, and these different runs were connected according to the neutron counts of the $^6$Li-glass counter. Therefore, any possible systematic changes in experimental conditions could be corrected for. Here a blank run was made in order to determine the background (discussed later) and also to monitor any changes in the incident neutron energy and the thickness of the $^7$Li neutron production target.

The spectrometer was shielded with various materials; $^6$LiH and borated paraffin played a major role to attenuate the intensity of the neutrons scattered by the sample (and various materials in the experimental room), thus preventing the neutrons from entering the NaI(Tl) spectrometer. A poor neutron shield would produce a large $\gamma$-ray and $\beta$-ray background from both the $^{127}I(n,\gamma)^{128}I$ reaction and the produced activity of $^{128}$I, respectively, and thus would make hard to extract a small true signal from these background. Here it should be noted that the $(n,\gamma)$ cross section increases generally with decreasing the neutron energy, and therefore, the scattered neutrons were likely to be captured by the various elements near to the NaI(Tl) spectrometer, producing the background. In order to attenuate the (external) background, including the $\gamma$ rays from natural radioactivities of $^{40}$K, $^{208}$Tl, etc., Pb was used.

The spectrometer was already known to have high sensitivity to the prompt $\gamma$-ray detection from the neutron-capture reaction at low $E_n \leqslant 80$ keV [18], but it has not been well studied at high $E_n$. Here the low-energy neutrons were emitted from the Li target within a narrow cone with respect to the proton beam direction; therefore, they did not hit the spectrometer directly and thus the above-mentioned shield was good enough to attenuate the events due to the scattered neutrons. However, when the neutron energy becomes high, $\sim$500 keV, the neutrons are emitted to all directions, and, thus, the neutrons can collide directly with the hydrogen in the shield materials of the borated paraffin and/or $^6$LiH in the spectrometer, thus producing background $\gamma$ rays due to the $H(n,\gamma)d$ reaction. If such an event occurs, it becomes difficult to discriminate the true event due to the polyethylene sample from the background by the TOF method, since the distance between the Li target and the borated paraffin and/or $^6$LiH is almost same as that between the Li target and the sample. Actually, we observed such a $\gamma$-ray event from the $p(n,\gamma)d$ reaction without the polyethylene sample in the same experimental setup as the low-$E_n$ one; we thus made efforts to reduce the background by using various shadow bars and shield materials (Pb and borated paraffin) surrounding $^6$LiH with different shapes and compositions. The shadow bar was used mainly to attenuate the intense high-energy $\gamma$ rays from the $^7Li(p,\gamma)^8Be$ reaction. After extensive studies, we could reduce not only the background, but also the scattered neutrons from the sample with the experimental setup as shown in Fig. 2. One of the essential points was that the thickness of Pb surrounding $^6$LiH must be thin; otherwise, the scattered neutrons from the sample could stream into the NaI(Tl) detector through Pb, producing the $\gamma$-ray background up to 6.8 MeV from the $^{128}I(n,\gamma)^{128}I$ reaction in the detector [23].

The spectrometer was set at 125.3°, where the second Legendre polynomial is zero and therefore, the $\gamma$-ray intensity measured at this angle gives an angle-integrated $\gamma$-ray intensity for the dipole transition.

## III. RESULTS AND DISCUSSION

The TOF spectra measured for Au and polyethylene by the central NaI(Tl) detector are shown in Fig. 4, where the peaks at about 440 and 390 channels for Au were due to the $\gamma$ rays from the $^7Li(p,\gamma)^8Be$ and $^{197}Au(n,\gamma)^{198}Au$ reactions by the 550-keV neutrons, respectively. Although these peaks were well separated from each other, the tail of the former reaction contributed to the latter peak, and therefore caused the continuous $\gamma$-ray background in the background-subtracted spectrum (discussed below). The foreground (FG) and background (BG) $\gamma$-ray spectra obtained by putting the gates on the $F$ and $B$ regions in the above TOF spectrum are shown for the 6.3-mm-thick sample in Fig. 5 as thick and thin lines, respectively. The background-subtracted (BS) $\gamma$-ray spectrum is shown in Fig. 6 as a solid point, where we still see continuous background, which was mostly due to the $\gamma$ ray from the $^7Li(p,\gamma)^8Be$ reaction at the Li target. In order to subtract the background, we measured the $\gamma$-ray

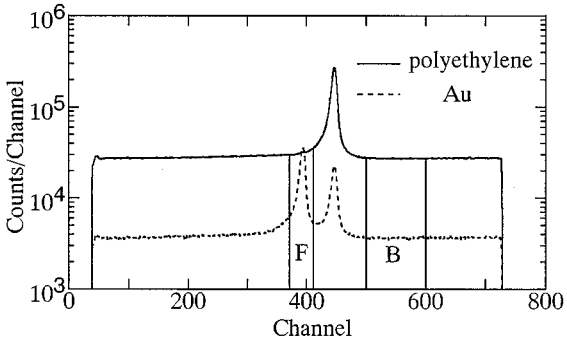


FIG. 4. TOF spectra measured by a central NaI(Tl) detector using gold (dotted line) and polyethylene (solid line) samples, respectively. Here foreground (including background) and background spectra can be obtained by setting the gates on the *F* and *B* regions in the spectrum, respectively.

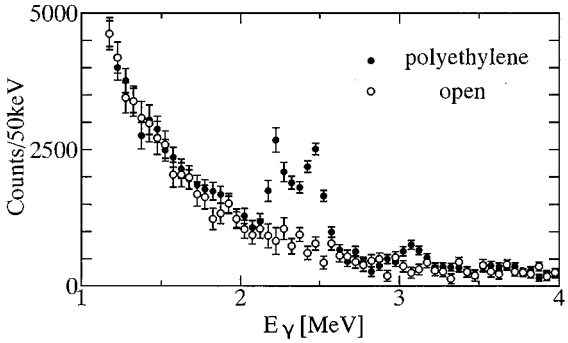


FIG. 6. Background-subtracted (BS) spectra obtained by subtracting the background spectrum from the foreground one measured with a polyethylene sample (solid circle) and without the sample (open circle), respectively. The continuous spectrum shown by the open circle was due to the $^{7}$Li$(p,\gamma)^{8}$Be reaction at the neutron production target.

spectrum without the sample, which is shown in Fig. 6 as an open point. The net spectrum, obtained by subtracting the continuous spectrum from the BS spectrum, is shown in Fig. 7. The $\gamma$-ray energy was calibrated by using the $\gamma$-ray standard sources, the background $\gamma$-ray peaks of 1.461 MeV ($^{40}$K) and 2.615 MeV ($^{208}$Tl) and the $\gamma$ rays from the $^{56}$Fe$(n,\gamma)^{57}$Fe reaction, respectively. Iron was used to cover the spectrometer.

In Fig. 7 two broad peaks of 2.50 and 2.22 MeV are due to the $p(n,\gamma)d$ reactions induced by the 550-keV incident neutrons and the neutrons decelerated by multiple scattering by hydrogen and/or carbon atoms in the polyethylene sample, respectively. Here something should be mentioned about the shape and peak energy of the 2.22-MeV $\gamma$ ray. Since the $\gamma$-ray energy from a thermal neutron capture by a proton is 2.225 MeV, one may wonder that the above 2.22-MeV $\gamma$ ray could be due to the neutrons thermalized by the multiple scattering of the incident neutrons by various materials in the experimental room. The events due to these neutrons, could be discriminated by the TOF and therefore they should not appear in the background-subtracted (net) spectrum; actually, the $\gamma$ rays from the $^{56}$Fe$(n,\gamma)^{57}$Fe reaction caused by the thermalized neutrons are not observed in the spectrum, while the events due to the decelerated neutrons in the polyethylene sample could not be discriminated with the TOF method, since the deceleration of the incident neutrons would proceed within a few nsec because of the thin polyethylene sample. The following two factors might be the reason why one sees the 2.22-MeV $\gamma$-ray peak. First, the neutron has the same mass as the proton, and second, the neutron-capture cross section increases with decreasing the neutron energy. Namely, when the neutron collides with the proton (H) in the sample, it loses half of the incident energy; after several collisions, the neutron energy becomes so small that the neutron is likely to be captured by the proton. As discussed later, the 2.22-MeV peak was fitted quite well by the calculation based on the scattering process, and thus, hereafter, we assume the decelerated neutron to be the thermal one for simplicity.

The 3.09-MeV peak is the $\gamma$ ray decaying from the first-excited (3.09-MeV) state of $^{13}$C, populated by the $^{12}$C$(n,\gamma)^{13}$C reaction in the sample, to the ground state [24] (see the partial level scheme of $^{13}$C in Fig. 8). Therefore one should see the $\gamma$ ray decaying from the capture state to the 3.09-MeV state, whose energy is 2.37 MeV for the 550-keV neutrons, just between the 2.22- and 2.50-MeV peaks. (The $\gamma$-ray energy is 1.86 MeV for thermal neutrons [24].) Therefore, in order to determine the $p(n,\gamma)d$ cross section by analyzing the 2.50-MeV peak intensity it is better to know the 2.37-MeV $\gamma$-ray intensity, which is discussed below. Here, if the 3.09-MeV $\gamma$ ray would be only due to the 550-keV neutrons, the 2.37-MeV intensity would be equal to the 3.09-MeV one within an uncertainty of 4%, which was ob-

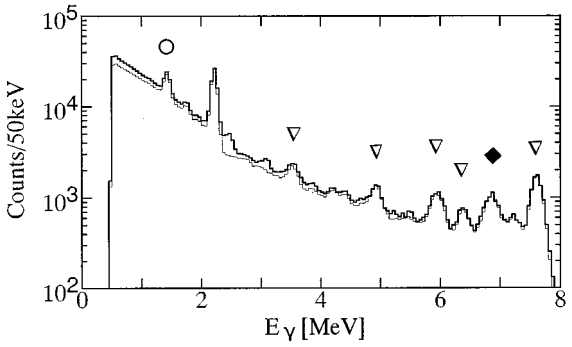


FIG. 5. (a) Foreground (thick) and (b) background (thin) $\gamma$-ray spectra for a polyethylene sample obtained by setting the gates on the *F* and *B* regions in Fig. 4, respectively.

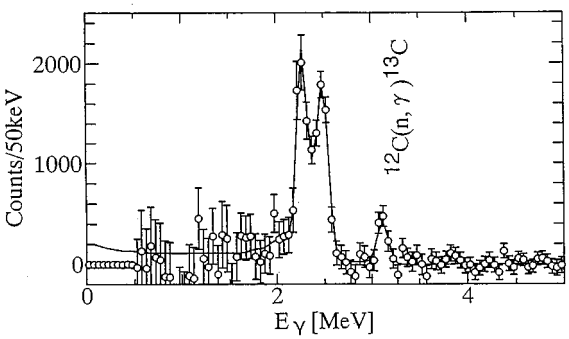


FIG. 7. Net spectrum obtained by subtracting the continuous spectrum from the BS one.

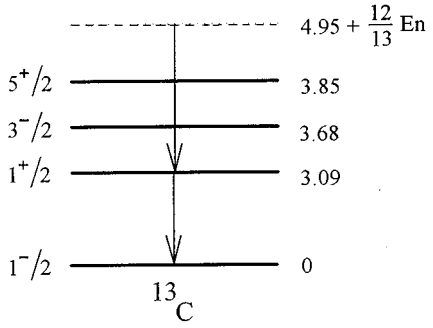


FIG. 8. Partial level scheme of $^{13}C$.

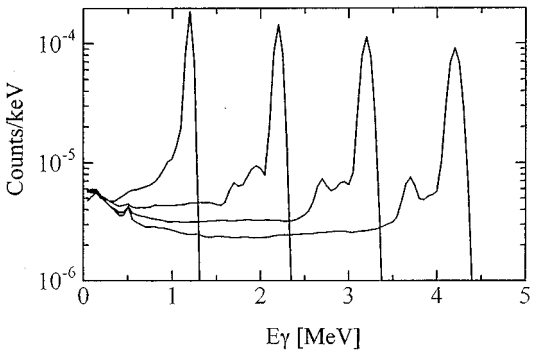


FIG. 9. Gamma-ray response function of the NaI(Tl) detector.

tained by the recent measurements of the $^{12}C(n,\gamma)^{13}C$ reaction cross section at $E_n=550$ keV [25]. In the present experiment the above peaks of 2.22 and 2.50 MeV were due to the $p(n,\gamma)d$ reaction in the polyethylene sample; therefore, one might think that both the decelerated and 550-keV neutrons would be captured by $^{12}C$, and thus, they contributed to populate the 3.09-MeV state in $^{13}C$. If so, one has to know the 3.09-MeV $\gamma$-ray intensity due to the 550-keV neutrons to derive the 2.37-MeV one. The decelerated neutrons, however, did not contribute to populate the 3.09-MeV state. This is because the partial capture cross section populating the state is small for thermal neutrons, 14.1 $\mu$b [24], and is almost the same for the 550-keV neutrons, 24.1 $\mu$b [25], while the $p(n,\gamma)d$ reaction cross section is $\sim 10^4$ times larger for thermal neutrons, 334.2 mb [4], than that for the 550-keV neutrons, 35.2 $\mu$b (discussed later). Therefore, the decelerated neutrons played a minor role to populate the capture state in the $^{12}C(n,\gamma)^{13}C$ reaction, although they played the important role in the $p(n,\gamma)d$ reaction. The interpretation is consistent with the nonobservation of the 4.95-MeV $\gamma$ ray, decaying from the capture state of $^{13}C$ to the ground state (Fig. 7). Namely, the partial capture cross section for the $\gamma$ ray is 2.3 mb for thermal neutrons [24] and it is about 160 times larger than that for the 1.86-MeV $\gamma$ ray [24]. Therefore, if the decelerated neutrons could play important roles in the $^{12}C(n,\gamma)^{13}C$ reaction, we should observe the 4.95-MeV $\gamma$ ray. Consequently, the 2.37-MeV $\gamma$-ray intensity, being equal to the 3.09-MeV one, was obtained reliably using the measured 3.09-MeV $\gamma$-ray one. Gamma-ray intensities connecting between discrete levels, and between a capture state and a low-lying discrete level, were analyzed, respectively, as follows. Namely, in the former case, the $\gamma$-ray intensity was obtained by a stripping method, using the response function of the NaI(TI) detector, which was obtained experimentally as shown in Fig. 9 [20], while in the latter case, the shape of the $\gamma$-ray spectrum was different from that of the former one due to energy spread of the incident neutrons produced by the $^7Li(p,n)^7Be$ reaction and of the multiple-scattering events of the neutrons in the sample, respectively. The two peaks of 2.22 and 2.50 MeV in Fig. 7 are due to these effects as discussed above. Here the spread of the incident neutrons was mostly due to the straggling of the proton beam in the Li target, while the spread due to the multiple-scattering events is quite important in the present polyethylene sample. Here it should be added that the incident neutron decreases the energy also by colliding with the carbon in the sample. In this case the energy loss is small, and therefore the scattering causes small energy change of the neutron. In order to analyze the above $\gamma$-ray spectra we made the Monte Carlo calculation by using a newly developed code TIME-MULTI [18], together with the above-mentioned stripping method. The measured incident neutron spectrum in Fig. 3 was convoluted to the response function. The spectrum thus fitted is shown in Fig. 7 as a solid line, where the above estimated intensity of the 2.37-MeV $\gamma$ ray was used. (The $\gamma$-ray intensities of 2.50, 2.37, and 2.22 MeV were obtained also by fitting the measured spectrum using the TIME-MULTI. The 2.37-MeV intensity thus obtained is in good agreement with the estimated one). In a similar way, the $\gamma$-ray intensities for a 10.5-mm-thick sample were analyzed.

The absolute cross section $\{\sigma_\gamma(n,\gamma)\}$ of the $p(n,\gamma)d$ reaction was obtained by using the $\gamma$-ray intensity $Y_\gamma(p)$ as

$$\sigma(n,\gamma)=C\,\frac{(r^2n)_{\mathrm{Au}}}{(r^2n)_p}\,\frac{\varphi(\mathrm{Au})}{\varphi(p)}\,\frac{Y_\gamma(p)}{Y_\gamma(\mathrm{Au})}\,\sigma_\gamma(\mathrm{Au}), \tag{1}$$

$$C=\frac{(C_{nm}C_{ns}C_{\gamma a}C_{\gamma g})_{\mathrm{Au}}}{(C_{nm}C_{ns}C_{\gamma a}C_{\gamma g})_p}. \tag{2}$$

Here $\varphi$ and $\sigma_\gamma(\mathrm{Au})$ are the relative neutron fluence and the absolute capture cross section of Au, respectively; $r$ and $n$ are the radius and thickness (atoms/b) of the sample, respectively. $Y_\gamma(\mathrm{Au})$ is the total capture yield obtained from the capture $\gamma$-ray spectrum of Au by using a pulse-height weighing technique [26]. $C$ is a correction factor comprising four factors ($C_{nm}$, $C_{ns}$, $C_{\gamma a}$, and $C_{\gamma g}$), as defined in Eq. (2). Here $C_{nm}$ is introduced to correct for the multiple-scattering effect of the incident neutron in the sample. Namely, it corrects for overestimation of the $\gamma$-ray yield due to the neutrons scattered in the sample, and thus it is defined as

$$C_{nm}=\frac{\text{total number of captured events}}{\text{number of captured events by the primary neutron}}. \tag{3}$$

$C_{ns}$ is introduced to correct for the shielding of the incident neutrons in the sample, since the flux of the incident neutron

TABLE I. Correction factors used in the data analysis. The correction factors of $C_{\gamma a}$ and $C_{\gamma g}$ for a polyethylene sample were included in the response function of the NaI(Tl) detector, and therefore they are not shown here.

| Sample | Thickness (mm) | $C_{nm}$ | $C_{ns}$ | $C_{\gamma a}$ | $C_{\gamma g}$ |
|---|---|---|---|---|---|
| Polyethylene | 6.3 | 1.15 | 0.83 | | |
| Polyethylene | 10.5 | 1.14 | 0.73 | | |
| Au | 1.0 | 1.08 | 0.98 | 0.92 | 1.00 |

is attenuated due to scattering and/or absorption in the sample. In order to calculate $C_{ns}$, an averaged neutron flux in the sample, $\phi$, is used, and it is defined as

$$\overline{\phi} = \int_0^d \{\phi \exp(-\rho\sigma_{\rm tot}x)dx\} \Big/ \int_0^d dx$$
$$= \{1-\exp(-\rho\sigma_{\rm tot}d)\}\phi/(\rho\sigma_{\rm tot}d). \quad (4)$$

Here $\phi$, $d$, $\rho$, $\sigma_{\rm tot}$ are the flux of the incident neutron, thickness (cm) and density (atoms/b/cm) of the sample, and the total cross section, respectively. Since $n$ is equal to $\rho d$, $\phi$ is given as follows:

$$\overline{\phi} = \{1-\exp(-n\sigma_{\rm tot})\}\phi/(n\sigma_{\rm tot}). \quad (5)$$

Thus the number of the capture neutron events, $Y$, in the energy region between $E$ and $E+dE$ is given as

$$Y(E)dE = n\sigma_c\overline{\phi}dE, \quad (6)$$

where $\sigma_c$ is the neutron-capture cross section at the neutron energy of $E$. The number of the captured neutron events, therefore, is obtained as

$$Y = \int n\sigma_c\overline{\phi}\,dE. \quad (7)$$

Here $C_{ns}$ is introduced as follows:

$$Y = C_{ns}\int n\sigma_c\phi dE. \quad (8)$$

It can be calculated as

$$C_{ns} = \int \sigma_c\overline{\phi}dE \Big/ \int \sigma_c\phi dE$$
$$= \int [\sigma_c\{1-\exp(-n\sigma_{\rm tot})\}/(n\sigma_{\rm tot})\phi dE] \Big/ \int \sigma_c\phi dE. \quad (9)$$

$C_{nm}$ and $C_{ns}$ were calculated using TIME-MULTI [18]. A detailed description of the code is found in Ref. [18]. $C_{\gamma a}$ and $C_{\gamma g}$ factors are for the $\gamma$-ray absorption by the sample and the finite size of the sample, respectively, and they were calculated by a Monte Carlo method. The correction factors thus calculated are shown in Table I. Finally, the cross sections were obtained as 35.9 (35) and 34.5 (32) $\mu$b for samples of 6.3 and 10.5 mm thickness, respectively, as shown in Table II. The quoted error consists of the statistics of the $\gamma$-ray yield, the response function, the absolute cross section of Au, and the extrapolation of the $\gamma$-ray yields of Au to the low-energy side. By averaging these values, we obtained a cross section of 35.2 (24) $\mu$b at 550 keV, which agrees well with the theoretical value of 36 $\mu$b by Sato *et al.* and differs by about 15% from the value derived from the inverse reaction at the corresponding neuron energy of 550 keV.

TABLE II. Cross section $\sigma$ of the $p(n,\gamma)d$ reaction measured at the averaged neutron energy of $E_n$=550 keV (laboratory). $\Delta E$ is the neutron energy width.

| Sample thickness (mm) | $E_n$ ($\Delta E$) (keV) | $\sigma$ ($\mu$b) |
|---|---|---|
| 6.3 | 550(33) | 35.9±3.5 |
| 10.5 | 550(33) | 34.5±3.2 |
| | | Average=35.2±2.4 |

Here one may wonder about the interference of the $M1$ and $E1$ transitions of the 2.5-MeV $\gamma$ ray from the $p(n,\gamma)d$ reaction. The interference, however, would not occur at the present $\gamma$-ray energy, where one can rely on the long-wave approximation. According to the approximation, the intrinsic spin of the scattering state of the neutron and proton is coupled into triplet and singlet states for the $E1$ and $M1$ $\gamma$-ray transitions, respectively. Here, although the $M1$ transition operator contains the spin operator, the $E1$ operator does not contain it. Therefore, the interference term becomes zero after summing over all possible spin states of the neutron. (Note that neutrons were unpolarized.) Thus the present cross section obtained by using the $\gamma$-ray intensity measured at 125.3° is the total one. Higher multipoles than $E2$ and $M2$ were calculated to be negligibly small [15].

Here it would be nice if we could find any possible reason in the discrepancy between the previous measurement of the $d(\gamma,p)n$ cross section and the present result. One possible reason might be due to a theoretical uncertainty of the photoelectric cross section (hereafter $\sigma_{\rm ph}$) for the $K$ shell in Pb. The cross section of the $d(\gamma,p)n$ reaction was measured by using the 2.51-, 2.62-, and 2.75-MeV $\gamma$ rays from the decays of $^{24}$Na, $^{208}$Tl, and $^{72}$Ga, respectively [16]. In the measurement, the absolute intensities of these $\gamma$ rays were calibrated by measuring the photoelectron intensities from the $K$shell emitted from a thin Pb foil, and therefore it was necessary to know $\sigma_{\rm ph}$. However, since the experimental value of $\sigma_{\rm ph}$ was not known at that time, the theoretical values of 1.252, 1.184, and 1.113 b were used for the 2.51-, 2.62-, and 2.75-MeV $\gamma$ rays, respectively [16]. After this experiment $\sigma_{\rm ph}$ for the $K$ shell in Pb was measured to be 0.93 (3) b for the 2.75-MeV $\gamma$ ray [27], about 15% smaller than the theoretical value. If we reduce the theoretical values by 15%, the cross sections thus renormalized agree quite well with the theoretical ones by Sato *et al.* Thus the theoretical uncertainty of $\sigma_{\rm ph}$ for the $K$ shell in Pb may be one of the major reasons for the discrepancy.

The discrepancy between experiment and theory still remains for the polarization $P(n)$ and angular distribution of

$P(n)$ of the neutron from the deuteron photodisintegration. In order to resolve the problem we are preparing another experiment [28].

Here it should be stressed that the neutron cross section by a proton at 550 keV is very sensitive to the $M1$ and $E1$ matrix elements, and also to the meson-exchange currents. The present study, therefore, demonstrates that the low-energy neutron-capture reaction by a proton is a unique probe for investigating the above effects. The experimental study of the $d(\gamma,p)n$ reaction near the threshold energy may not be feasible because of the detection difficulty of the emitted proton (neutron).

## ACKNOWLEDGMENTS

We acknowledge Prof. H. Ohtsubo and Prof. T. Sato for useful discussions. This work was supported by a Grant-in-Aid for Specially Promoted Research of the Japanese Ministry of Education, Science, Sports, and Culture.

[1] H. A. Bethe and C. Longmire, Phys. Rev. **77**, 647 (1950); N. Austern and E. Rost, *ibid.* **117**, 1506 (1959).
[2] R. V. Wagoner, W. A. Fowler, and F. Hoyle, Astrophys. J. **148**, 3 (1967); D. N. Schramm and R. V. Wagoner, Annu. Rev. Nucl. Part. Sci. **27**, 37 (1977).
[3] D. O. Riska and G. E. Brown, Phys. Lett. **38B**, 193 (1972).
[4] A. E. Cox, S. A. R. Wynchank, and C. H. Collie, Nucl. Phys. **74**, 497 (1965).
[5] J. Tudoric-Ghemo, Nucl. Phys. **A92**, 233 (1967); M. Bosman *et al.*, Phys. Lett. **82B**, 212 (1979).
[6] J.-H. Mathiot, Phys. Rep. **173**, 63 (1989).
[7] E. Hadjimichael, Phys. Lett. **46B**, 147 (1973); H. Arenhovel, W. Fabian, and H. G. Miller, *ibid.* **52B**, 303 (1974); M. L. Rustgi, R. D. Nunemaker, and R. Vyas, Can. J. Phys. **62**, 1064 (1984).
[8] R. J. Holt, K. Stephenson, and J. R. Specht, Phys. Rev. Lett. **50**, 577 (1983).
[9] R. W. Jewell *et al.*, Phys. Rev. **139**, B71 (1965).
[10] J. P. Soderstrum and L. D. Knutson, Phys. Rev. C **35**, 1246 (1987).
[11] F. D. Smit and F. D. Brooks, Nucl. Phys. **A465**, 429 (1987).
[12] W. A. Fowler, G. R. Caughlan, and B. A. Zimmerman, Annu. Rev. Astron. Astrophys. **5**, 525 (1967).
[13] G. M. Hale, D. C. Dodder, E. R. Siciliano, and W. B. Wilson, ENDF/B-VI, evaluation, material 125, revision 1 (1991).
[14] M. S. Smith, L. H. Kawano, and R. A. Malaney, Astrophys. J., Suppl. Ser. **85**, 219 (1993).
[15] T. Sato, M. Niwa, and H. Ohtsubo, in *Proceedings of the International Symposium on Weak and Electromagnetic Interactions in Nuclei*, edited by H. Ejiri, T. Kishimoto, and T. Sato (World Scientific, Singapore, 1995), p. 488.
[16] G. R. Bishop *et al.*, Phys. Rev. **80**, 211 (1950).
[17] T. S. Suzuki, Y. Nagai, T. Shima, T. Kikuchi, H. Sato, T. Kii, and M. Igashira, Astrophys. Lett. **439**, L59 (1995).
[18] K. Senoo, Y. Nagai, T. Shima, T. Ohsaki, and M. Igashira, Nucl. Instrum. Methods Phys. Res. A **339**, 556 (1994).
[19] H. Komano, Ph.D thesis, Tokyo Institute of Technology, 1984.
[20] M. Igashira, K. Tanaka, and K. Masuda, in *Proceedings of the 8th International Symposium on Capture Gamma-ray Spectroscopy and Related Topics*, Fribourg, Switzerland, edited by J. Kern (World Scientific, Singapore, 1994), p. 992.
[21] T. Ohsaki, Y. Nagai, M. Igashira, and T. Shima (unpublished).
[22] ENDF/B-VI, data file for 197 Au (Mat=792), evaluated by S. F. Mughabghab.
[23] L. A. Schaller, J. Kern, and B. Michaud, Nucl. Phys. **A165**, 415 (1971).
[24] F. Ajzenberg-Selove, Nucl. Phys. **A523**, 1 (1991).
[25] T. Kikuchi, Y. Nagai, T. Shima, T. Kii, T. Kobayashi, T. Baba, and M. Igashira (unpublished).
[26] R. L. Macklin and H. Gibbons, Phys. Rev. **159**, 1007 (1967).
[27] E. J. Bleeker, P. F. A. Goudsmit, and C. De Vries, Nucl. Phys. **29**, 452 (1962).
[28] T. Kii, T. Shima, T. Baba, T. Takahasi, and Y. Nagai (unpublished).